View Article Online / Journal Homepage / Table of Contents for this issue
Soft Matter
Dynamic Article Links

Cite this: *Soft Matter*, 2011, **7**, 5176

www.rsc.org/softmatter

PAPER

Realization of a lateral directional order in nematic and smectic A phases of rodlike molecules by using perfluoroarene–arene interactions†

Keiki Kishikawa,* Sumihiro Aikyo, Seiji Akiyama, Takahiro Inoue, Masahiro Takahashi, Shiki Yagai, Hiroaki Aonuma and Shigeo Kohmoto

Received 9th December 2010, Accepted 22nd March 2011
DOI: 10.1039/c0sm01459a

In order to realize biaxial mesophases of straight rod-like molecules by introduction of lateral perfluoroarene–arene interactions, non-alkylated rod-like liquid crystalline compounds C_6X_5–COO–C_6Z_4–C_6Z_4–OOC–C_6Y_5, **F-BB-F** (X = Y = F, Z = H), **F-BB-B** (X = F, Y = Z = H), **B-BB-B** (X = Y = Z = H), **B-FF-B** (X = Y = H, Z = F), **F-FF-B** (X = F, Y =H, Z = F), and **F-FF-F** (X = Y = Z = F) were prepared, and their phase transition behaviors were investigated by polarized light optical microscopy (POM) and differential scanning calorimetery (DSC). From the one- and two-dimensional X-ray diffraction (1D- and 2D-XRD) studies of the nematic and smectic A phases of **F-BB-F**, it was clarified that the smectic A phase had a lateral directional order in the layer and the nematic phase had a cybotactic smectic A structure.

Introduction

Usual nematic liquid crystal (LC) phases (uniaxial nematic (N_u) phases) of the rod-like molecules are rotating rapidly around their molecular long axes, and only have one directional order in their molecular long axes and no directional order in their lateral directions. In contrast, the rotation movements in biaxial nematic (N_b) phases[1–5] are slower than those in N_u phases, and the molecules in N_b phases have lateral directional order in addition to the axial directional order. This phase was originally found in lyotropic LC systems,[6] and recently a few examples of lyotropic N_b phases were reported.[7] However, in thermotropic LC system, realization of N_b phases is still very difficult and the methodology has not been established yet. Some of the previously reported N_b phases were shown to be N_u phases after re-evaluation.[8,9] These days, many scientists in chemistry, physics, and materials science have been challenged to realize thermotropic N_b phases, because the phases have very unique order and a high potentiality for realization of high-responsive optical switching devices.[1,5] Shape-assisted approaches are thought to be effective to slow down the molecular rotation movement and to generate a lateral directional order. In those approaches, bent rod-,[9–11] plate-,[12] bone-,[13,14] spoon-,[15] pipette-like[16] molecules, and mixtures of rod- and disk-like molecules[17] were examined to bring about N_b phases. Liquid crystalline oligomers and polymers in which the mesogenic units were linked covalently were also used for generation of a lateral directional order.[18] It is known that shape-assisted approaches are also effective to generate biaxial smectic A phases[19] in which board- and bent rod-like molecules have a layer structure with biaxial order. However, those molecular shapes have a disadvantage in changing the directions of their short molecular axes because they have large excluded volumes during the switching process. In this study, in order to decrease the excluded volumes, we designed straight rod-like molecules to realize N_b and biaxial smectic A phases.

Our concept is shown in Fig. 1. We expect that a uniaxial mesophase of rod-like molecules (A) can be changed to a biaxial mesophase (B) by introducing a strong lateral face-to-face (or edge-to-edge) intermolecular interaction. Control of the directional order of their aromatic faces in addition to that of their molecular long axes generates biaxiality in a nematic phase. We selected the face-to-face perfluoroarene–arene (PFA···A)

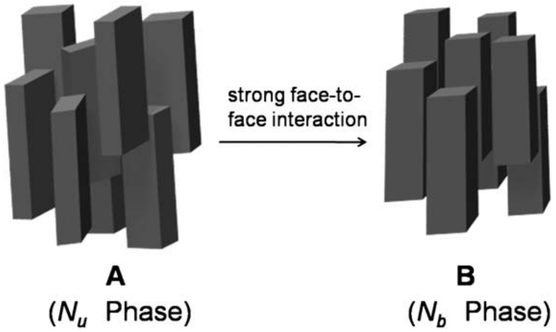

Fig. 1 A conceptual picture of the phase transformation from uniaxial mesophase (A) to biaxial mesophase (B) by introduction of the face-to-face attractive interaction.

Department of Applied Chemistry and Biotechnology, Faculty of Engineering, Chiba University, 1-33 Yayoi-cho, Inage-ku, Chiba, 263-8522, Japan. E-mail: kishikawa@faculty.chiba-u.jp; Fax: +81-43-290-3422; Tel: +81-43-290-3238

† Electronic supplementary information (ESI) available. See DOI: 10.1039/c0sm01459a

interaction[20] as the attractive interaction. The interaction is known as a strong attractive force between perfluorinated and non-fluorinated arenes which is composed of van der Waals and electrostatic interactions.[21] For example, the stabilization energy between benzene and hexafluorobenzene molecules was estimated to be 3.7–5.6 kcal mol^{-1} from both theoretical and experimental studies.[22,23] Recently, PFA···A interactions have mainly been used for crystal engineering,[24] and in some cases they are used for gel-formation,[25] double helix-formation,[26] self-assembly of polymers,[27] stereoselective synthesis[28] and molecular recognition.[29] The face-to-face interactions work only at a cofacial contact distance, because the main part of PFA···A interaction is dispersion energy which is proportional to r^{-6} (r: intercentroid distance between the two benzene rings). Accordingly, the molecular shape around the interaction site (π-face) should be sterically less-hindered so as not to suppress the intermolecular cofacial contacts, which makes the molecular design of LC compounds difficult. It forms a striking contrast to hydrogen bonding which only needs contact between –XH and Y (X, Y: hetero atoms) and is very useful for design of supramolecular LCs.[30] However, we believe that the features of PFA···A interaction, whose strength is proportional to r^{-6}, has an advantage during the switching process. The interaction sharply decreases when the faces of the two aromatic rings separate or become unparallel each other. Therefore, the rotations of the rodlike molecules around the long axis are not suppressed by intermolecular PFA···A interactions. On the other hand, rotations of bulky molecules are suppressed by the intermolecular steric repulsion during the entire rotation processes. From these reasons, we believe that this interaction-assisted approach has an advantage over shape-assisted approaches.

To the best of our knowledge, only one example is known to use this attractive interaction for stabilization of LC phases of rod-like molecules. Dai and co-workers reported that the 1 : 1 mixture of 1,4-di(phenylethynyl)benzene and the corresponding perfluorinated derivative and the 1 : 1 mixture of 1,4-di(phenylethynyl)-2,3,5,6-tetrafluorobenzene and 1,4-di(pentafluorophenylethynyl)benzene showed stable LC phases, though none of those pure compounds give a stable LC phase.[31] In non-calamitic mesophases, there are two examples of the stabilization of columnar LC phases using the PFA···A interaction. Grubbs' group reported a stable columnar LC phase of the 1 : 1 mixture of hexaalkoxytriphenylene and dodecafluorotriphenylene,[32] and our group reported stable columnar LC phases of trialkoxybenzyl pentaflurobenzoates possessing one pentafluorobenzene ring (PFB) and one non-fluorinated benzene ring (NFB) in their molecules.[33] Those examples suggested that the moiety ratio of 1 : 1 for PFBs and NFBs should be important for the generation of stable LC phases.

In this study, rod-like compounds **F-BB-F** and **B-FF-B** were designed based on our concept (Scheme 1). Our molecules have the following features to maximize the attractive interaction between the PFB and NFB; 1) the moiety ratio of PFBs/NFBs in the molecule is 1 : 1 to obtain the maximum intermolecular interaction, and 2) the molecules have no alkyl chain in order to avoid a decrease in intermolecular core–core interactions by steric repulsion between alkyl chains. Other compounds, **F-B-B-B**, **B-BB-B**, **F-FF-B** and **F-FF-F** were prepared to compare their behaviors with **F-BB-F** and **B-FF-B**.

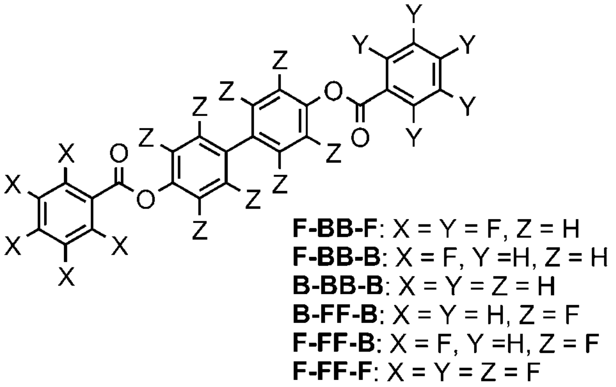

Scheme 1 Molecular structures of **F-BB-F**, **F-BB-B**, **B-BB-B**, **B-FF-B**, **F-FF-B** and **F-FF-F**.

By studying all the intermolecular interactions except the face-to-face PFA···A interaction, we estimated the following three attractive interactions in these LC phases; C–F···H–C interactions between the PFB and NFB,[34] F···F interactions between the two PFBs[35] and edge-to-face (C–H/π) interactions between two NFBs.[36] The C–F···H–C and F···F interactions interact as edge-to-edge interactions between molecules, which also assists the face-to-face arrangements of these molecules.[37] In contrast, the edge-to-face (C–H/π) interaction between two NFBs (less than 1 kcal mol^{-1}[36]) suppresses the face-to-face interaction, but it is much weaker than the PFA···A interaction. Accordingly, we expected that the benzene rings of the molecules should be arranged by PFA···A, C–F···H–C and F···F interactions in a face-to-face (and edge-to-edge) manner in the LC phases of **F-BB-F** and **B-FF-B**.

Results and discussion

Synthesis of the liquid crystalline compounds

Compounds **F-BB-F**, **F-BB-B** and **B-BB-B** were synthesized by condensation of 4,4′-biphenol and the corresponding carboxylic acids (pentafluorobenzoic acid and/or benzoic acid), respectively. With a similar procedure, **B-FF-B**, **F-FF-B** and **F-FF-F** were prepared from octafluoro-4,4′-biphenol and the corresponding carboxylic acids.

Phase identification and DSC of the compounds

The phases of the compounds were identified by POM, and their transition temperatures and enthalpies were investigated by DSC. Their phase behaviors are shown in Table 1. Compounds **F-BB-F** and **F-BB-B** showed nematic and smectic A phases. The non-fluorinated compound **B-BB-B** did not show any LC phase. Compounds **F-FF-B** and **F-FF-F** showed a nematic phase only on cooling. We expected that **B-FF-B** would give stable LC phases because of the 1 : 1 moiety ratio (PFBs/NFBs). However, it did not show any LC phase.

In the POM of the smectic A phases of **F-BB-F** and **F-BB-B**, fan-like textures with dark lines parallel to the directions of the crossed polarizers were observed and are the typical textures of smectic A phases (Fig. 2a)[38] which indicates that the phases had layer structures and the molecules were parallel to the layer

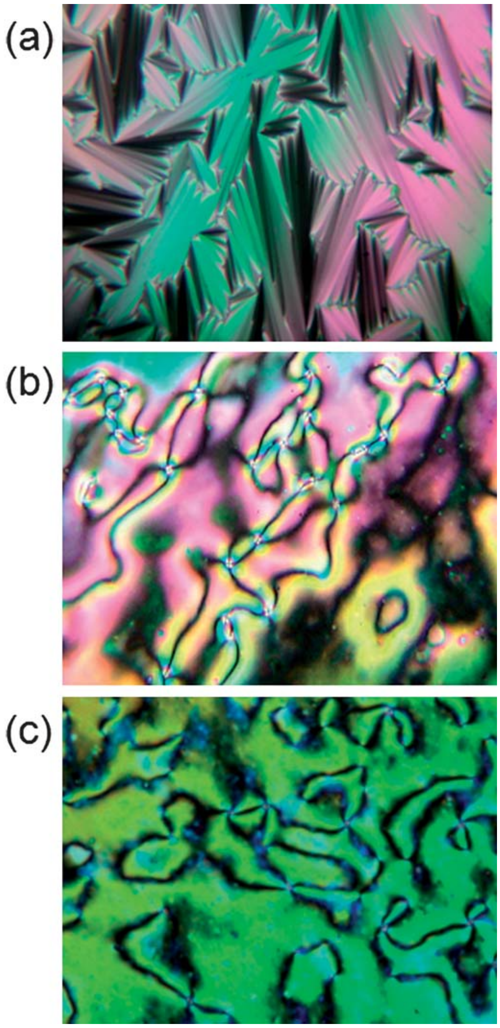

Fig. 2 Polarized optical micrographs of (a) fan-shaped texture of the smectic A phase of **F-BB-F** (190 °C, 600×), (b) schlieren texture of the nematic phase of **F-BB-F** (210 °C, 600×), and (c) schlieren texture of the nematic phase of **F-FF-F** (150 °C, 600×).

normal. The nematic phases of **F-BB-F**, **F-BB-B**, **F-FF-B** and **F-FF-F** exhibited schlieren textures with two and four-brushes (Fig. 2b) which are typical textures of nematic phases.[38] However, in the nematic phase of **F-BB-F**, each of the four-brushes has a small bright area at its center, and the lines are very sharp around the centers. It is known that the core can produce a bright texture if the inclined region is not too small. Further, both of the two- and four -brush disclinations have a different color area to that of their peripheral area (Fig. S1 and Fig. S2 in the ESI†). The changes of the colours mean that the refractive indices change significantly at the central areas of those disclinations. It strongly suggests that the molecular alignments greatly change in these areas even in the case of two-brush disclinations. This is in contrast to the schlieren texture of **F-FF-F** which has no bright area at the disclination and broad lines around them (Fig. 2c). At the transition from the smectic A phase to the nematic phase of **F-BB-F** on heating, smectic-like textures (fan-like and focal conic-like textures) remained after the transition up to the clearing temperature (Fig. S3†).

Table 1 Phase transition behaviours of the 4,4′-bis(benzoyloxy)-biphenyl derivatives[a]

Compound	Phase transition (°C, (kcal mol⁻¹))
F-BB-F	$\mathrm{Cr_1} \underset{102.7\ (-5.2)}{\overset{141.6\ (5.2)}{\rightleftharpoons}} \mathrm{Cr_2} \underset{173.6\ (-6.0)}{\overset{181.6\ (5.9)}{\rightleftharpoons}} \mathrm{SmA} \underset{203.7\ (-0.5)}{\overset{205.1\ (0.5)}{\rightleftharpoons}} \mathrm{N} \underset{246.9\ (-0.1)}{\overset{248.1\ (0.1)}{\rightleftharpoons}} \mathrm{Iso}$
F-BB-B	$\mathrm{Cr} \xrightarrow{188.7\ (h_1)^b} \mathrm{X} \xrightarrow{T^c\ (h_2)^b} \mathrm{N} \underset{262.7\ (-0.2)}{\overset{264.1\ (0.1)}{\rightleftharpoons}} \mathrm{Iso}$ $\mathrm{Cr} \xleftarrow[151.3\ (-7.9)]{} \mathrm{SmA} \xleftarrow[189.4\ (-0.3)]{} \mathrm{N}$
B-BB-B	$\mathrm{Cr} \underset{231.2\ (-8.3)}{\overset{251.5\ (8.3)}{\rightleftharpoons}} \mathrm{Iso}$
B-FF-B	$\mathrm{Cr} \underset{174.5\ (-10.5)}{\overset{184.0\ (10.3)}{\rightleftharpoons}} \mathrm{Iso}$
F-FF-B	$\mathrm{Cr} \xrightarrow{173.1\ (12.7)} \mathrm{Iso}$ $\mathrm{Cr} \xleftarrow[135.0\ (-12.7)]{} \mathrm{N} \xleftarrow[162\ (-0.1)]{} \mathrm{Iso}$
F-FF-F	$\mathrm{Cr} \xrightarrow{162.5\ (6.7)} \mathrm{Iso}$ $\mathrm{Cr} \xleftarrow[137.2\ (-6.9)]{} \mathrm{N} \xleftarrow[160\ (-0.1)]{} \mathrm{Iso}$

[a] The transition temperatures (°C) and enthalpies (in parentheses, kcal mol⁻¹) were determined by DSC (5 °C min⁻¹) and are given above and below the arrows. $\mathrm{Cr_1}$, $\mathrm{Cr_2}$ and Cr indicate crystal phases, and SmA, N, Iso, and X indicate smectic A, nematic, isotropic liquid and unidentified phases, respectively. [b] The peaks could not be separated. $h_1 + h_2 = 9.5$ kcal mol⁻¹. [c] The peaks were overlapping, and the transition temperature could not be measured.

Comparing the melting points of **F-BB-F** and **F-BB-B** with **B-BB-B** which possesses a biphenyl group, show that those of **F-BB-F** and **F-BB-B** were much lower than that of **B-BB-B**. The melting point of **F-BB-F** is lower than that of **F-BB-B**. Introduction of fluorine atoms on the benzoyl–benzene rings were effective in lowering the melting point. As for **B-FF-B**, **F-FF-B** and **F-FF-F** which possess an octafluorobiphenyl moiety, their melting points were lower than those of **B-BB-B**, **F-BB-B** and **F-BB-F**, respectively. The clearing temperatures of the nematic phases of **F-F-F-B** and **F-FF-F** were lower than those of **F-BB-B** and **F-BB-F**, respectively. The replacement of the biphenyl with an octafluorobiphenyl moiety was effective for lowering the melting and clearing points. To investigate the differences in their conformations, the density functional theory (DFT) calculations (B3LYP/6-31G(d))[39] were performed. The most stable conformations of **F-BB-F** and **B-FF-B** are shown in Fig. 3. The molecular shape of **F-BB-F** is flat, while that of **B-FF-B** is twisted. In the case of **F-BB-F**, the torsion angles between the two

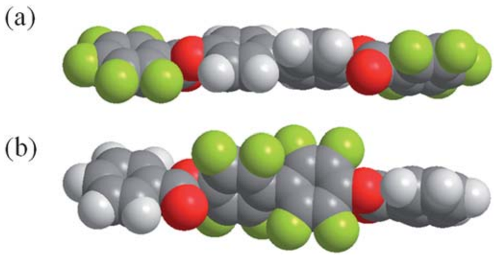

Fig. 3 Most stable conformers of (a) **F-BB-F** and (b) **B-FF-B** calculated by the DFT (B3LYP6-31G(d)) method.[39]

Table 2 The XRD peaks of **F-BB-F** and **F-BB-B** in the smectic A phases and their intensities

Compound	Mesophase[a](Temp/°C)	d_{obsd} (d_{calcd})/Å[b]	Miller index/(*hkl*)	Relative Intensity (%)	l_{calcd}/Å[e]
F-BB-F	SmA(190)	22.1 (22.1)	(100)	100[c]	24.2
		11.3 (11.1)	(200)	18[c]	
		7.5 (7.6)	(300)	6[c]	
	SmA(200)	23.6 (23.6)	(100)	25[d]	
		11.9 (11.8)	(200)	100[d]	
		7.9 (7.9)	(300)	10[d]	
F-BB-B	SmA(170)	23.4 (23.4)	(100)	15[d]	24.0
		11.8 (11.7)	(200)	100[d]	
		7.9 (7.8)	(300)	5[d]	
	SmA(190)	23.5 (23.5)	(100)	38[d]	
		11.8 (11.8)	(200)	100[d]	
		7.9 (7.8)	(300)	1[d]	

[a] SmA indicates a smectic A phase. [b] The values d_{obsd} and d_{calcd} indicate *d*-spacing observed in the XRD and *d*-spacing calculated based on the *d*(100) distance. [c] Percentage of the peak intensity divided by that of *d*(100). [d] Percentage of the peak intensity divided by that of *d*(200). [e] Molecular length calculated by Chem3D.[40]

benzene rings of the biphenyl group were about 38°. The π-faces of the biphenyl–benzene ring and benzoyl–benzene ring linked with the ester group were almost in the same plane (the torsion angle between them is about 2°). On the other hand, the angle of about 59° was obtained in **B-FF-B** between the two perfluorinated benzene rings of the octafluorobiphenyl. The torsion angle between the octafluorobiphenyl–benzene ring and benzoyl–benzene ring was about 88°. Because of the bulky molecular shape, the attractive face-to-face interaction between the **B-FF-B** molecules is thought to be weak. These results indicate that molecular flatness should be one of the important factors for generation of stable LC phases in this series.

1D-X-ray diffraction studies of F-BB-F and F-BB-B on a glass plate without applying a magnetic field

To investigate the molecular-packing structures in the smectic A phases of **F-BB-F** and **F-BB-B**, their one-dimensional X-ray diffraction (1D-XRD) profiles were measured (Table 2).

Each of the samples was prepared by spreading it on an untreated glass plate. The X-ray patterns of these mesophases gave reciprocal spacings in the ratio 1 : 2 : 3 corresponding to their lamellar structures. The smectic A phase of **F-BB-F** at 190 °C (Fig. 4a) shows a large sharp *d*(100) peak corresponding to its interlayer spacing. The intensity of the *d*(100) peak is much stronger than that of the *d*(200) peak. However, intensities of these peaks were reversed at 200 °C (Fig. 4b). The *d*(200) peak is more intense than that of the *d*(100). Further, the shape of the halo in the XRD at 200 °C is different from that at 190 °C. Though no textural change was observed by POM in the temperature range of the smectic A phase, the XRD profiles indicated the gradual change in the layer structures. The halos at both 190 and 200 °C have a maxima at $2\theta = 22$–$24°$ (3.9–3.8 Å) corresponding to the thickness of the aromatic rings. In general, smectic A and nematic phases of straight rod-like molecules consisting of plural benzene rings have a broad maximum at 4.5–4.8 Å corresponding to their average molecular width.[41] Accordingly, these results suggest that the free rotation of these rod-like molecules along their long axis is suppressed in the smectic A phase of **F-BB-F**, and the aromatic faces are stacked in a face-to-face manner and parallel to the glass surface.

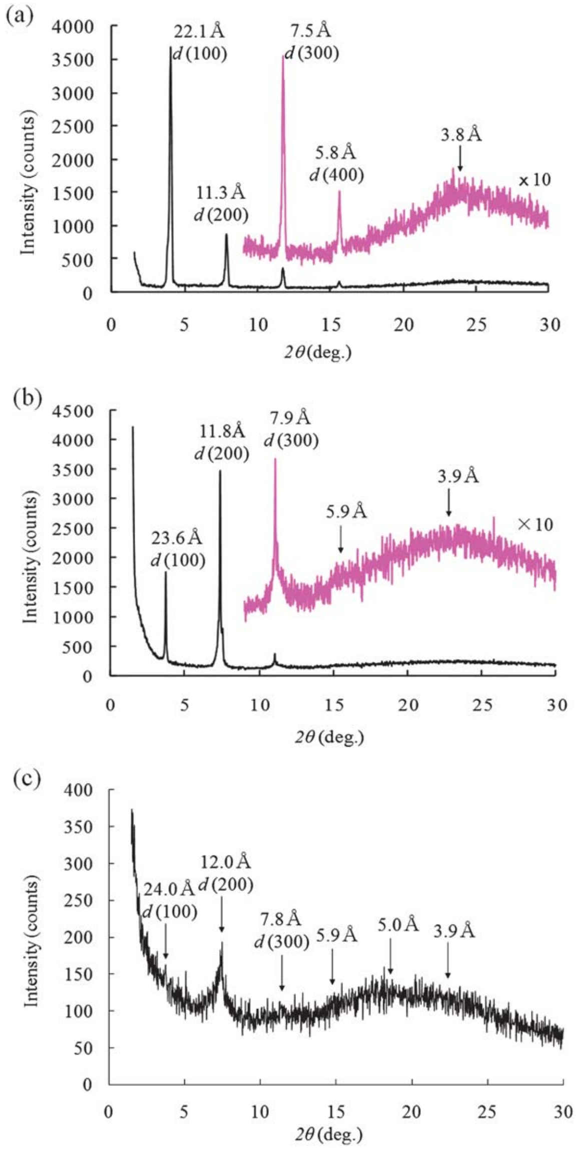

Fig. 4 1D-XRD profiles of **F-BB-F** at (a) 190 °C (smectic A phase), (b) 200 °C (smectic A phase) and (c) 210 °C (nematic phase).

The nematic phase of **F-BB-F** at 210 °C (Fig. 4c) did not show any peaks in the small angle region, and the shape of the halo became broader at the transition from the smectic A to the nematic phase. The XRD patterns of **F-BB-B** in its smectic A phase at both 170 and 190 °C showed that the *d*(200) peak was more intense than the *d*(100) peak. Therefore, it was assumed that the smectic A phase of **F-BB-B** maintained one packing structure over the observed temperature range.

2D-XRD studies with applying magnetic field

To obtain more information about the molecular-packing structures in the nematic and smectic A phases of **F-BB-F**, their two-dimensional X-ray diffraction (2D-XRD) profiles were measured on the samples sealed in a glass capillary ($\phi = 1.5$ mm). The molecules were aligned by applying a magnetic field (3500 gauss). The 2D-XRDs of the smectic A phases at 190 and 200 °C (Fig. 5a and Fig. 5b) showed pairs at the *d*(100) *d*(200), and *d*(300) reflections corresponding to their interlayer orders along the equator and the broad reflections corresponded to the averaged molecular widths at the meridian. These 2D-XRD patterns indicate that the molecular long axes are parallel to the layer normal. Further, in the nematic phase at 210 °C (Fig. 5c), pairs of reflections at *d*(200) and *d*(300) are observed along the equator in the small angle region, which indicates that the nematic phase also possesses a repeat distance in the direction of the molecular long axes. This means that the molecules are packed with a shift of the half molecular length in the level of small molecular aggregates, even though the textures in POM belonged to those of nematic phases. To investigate the influence of the PFA···A interaction, the 2D-XRD profile of **F-FF-F** was measured (Fig. 5d). The profile does not have a diffraction pattern which corresponding to a layer structure, and only shows a halo corresponding to the molecular width. Accordingly, the difference between the nematic phases of **F-BB-F** and **F-FF-F** suggests that the PFA···A interaction is necessary to generate the cybotactic smectic layer structure in the nematic phase of **F-BB-F**.

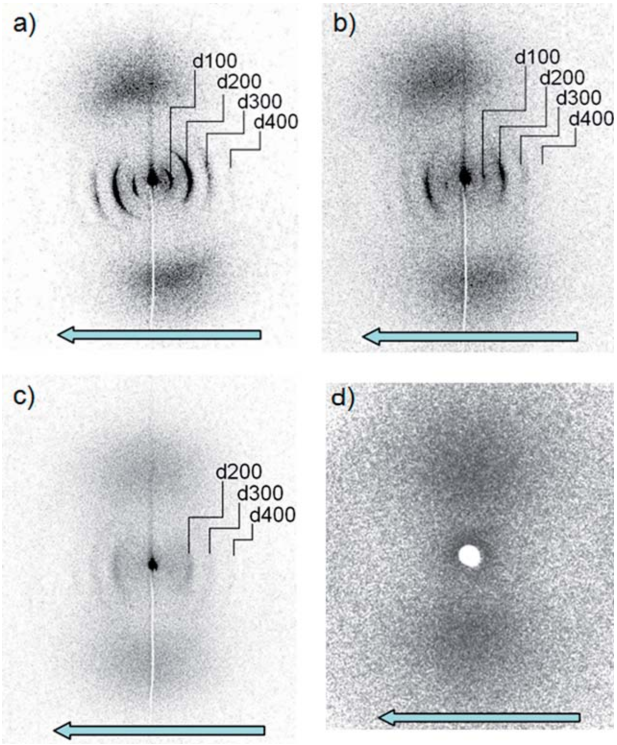

Fig. 5 2D-XRD patterns of (a) **F-BB-F** at 190 °C (smectic A phase), (b) **F-BB-F** at 200 °C (smectic A phase), (c) **F-BB-F** at 210 °C (nematic phase) and **F-FF-F** at 150 °C (nematic phase). The direction of the magnetic field is indicated by an arrow.

Crystal structure of F-BB-F

Single crystals of **F-BB-F** were obtained by recrystallization from chloroform–hexane solution, and the single crystal XRD of **F-BB-F** were performed to give the molecular packing structure in the crystal phase as shown in Fig. 6. In Fig. 6a, the C_6F_5– groups are stacked in an orderly fashion with a repeat distance of 3.2 Å. The molecules are packed in such a way that the PFBs and NFBs are micro-segregated in a layer as shown in Fig. 6b. It was assumed that CH/π interaction between the biphenyl moieties

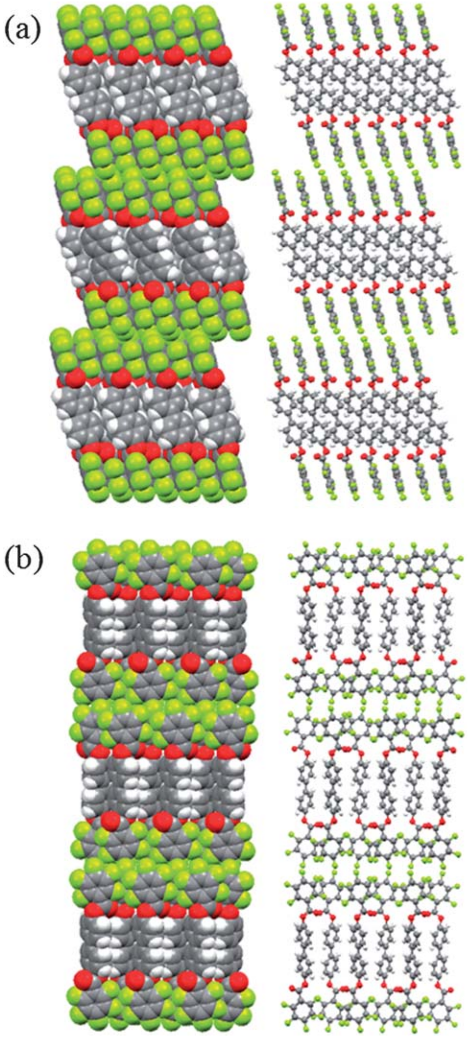

Fig. 6 Molecular packing structure (space-fill and ball-and-stick models) of **F-BB-F** in the crystal phase. Its (a) side and (b) front views.

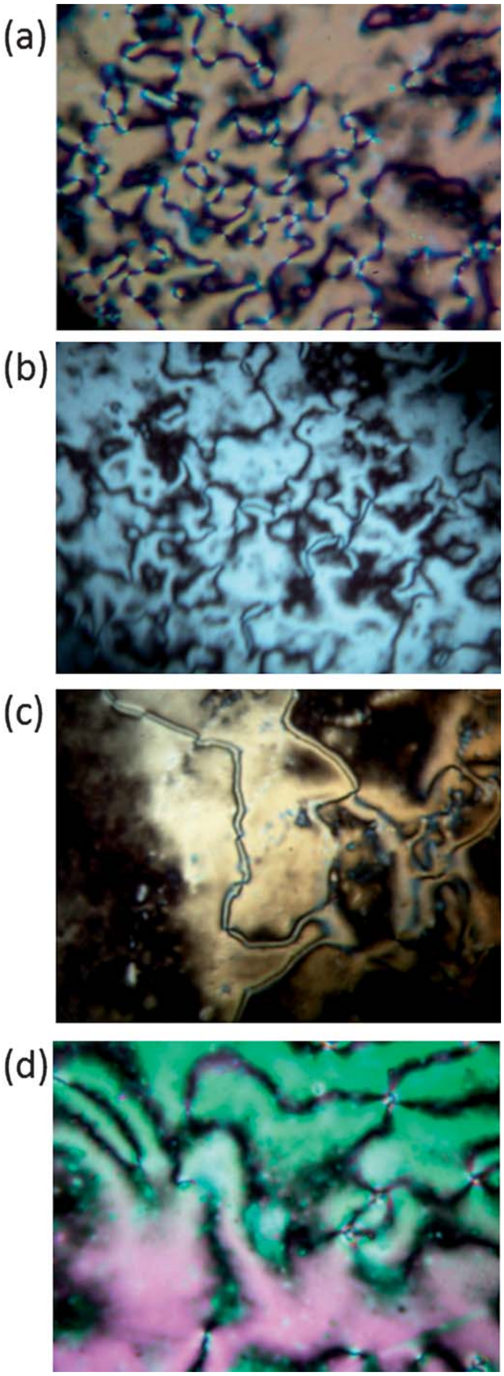

Fig. 7 Dark schlieren textures in the nematic phases of (a) **F-BB-F** (210 °C), (b) 4-cyano-4′-octylbiphenyl (**8CB**) (30 °C), (c) *N*-(4-ethoxybenzylidene)-4-*n*-butylaniline (**EBBA**) (76 °C), and (d) **F-FF-F** (150 °C). The samples were observed under a magnetic field (3500 gauss) between two glass plates treated with 1,1,1,3,3,3-hexamethyldisilazane.

and the F···F interactions between the NFBs took place during the crystallization process. The F···F interaction should be the main intermolecular interaction because each fluorine atom contacts efficiently with the fluorine atoms of other molecules. It is assumed that this edge-to-edge interaction organizes the π-faces of the PFBs in parallel in the crystal phase. The layer structure is almost the same as that estimated from the 1D-XRD of **F-BB-F** at the lower temperature region of its smectic A phase.

POM and 1D-XRD of F-BB-F on applying a magnetic field

To investigate the biaxiality of the nematic phase of **F-BB-F**, POM was performed on the nematic phase homeotropically aligned by applying a magnetic field (3500 gauss). Compound **F-BB-F** was sandwiched between two glass plates whose surfaces were treated with 1,1,1,3,3,3-hexamethyldisilazane to decrease interactions between molecules and the glass surface. Surprisingly, under the magnetic field, the nematic phase showed dark schlieren textures with all-two-brush disclinations (Fig. 7a), although it showed bright schlieren textures with two- and four-brush disclinations in the sample sandwiched between two untreated glass plates in the absence of a magnetic field (Fig. 2b). In this case, each of the two-brush declinations also has a small bright area as shown in the 4-brush textures in Fig. 2b. In order to compare the textures of **F-BB-F** with those of other nematic liquid crystalline compounds, the textures of 4-cyano-4′-octylbiphenyl (**8CB**) and *N*-(4-ethoxybenzylidene)-4-*n*-butylaniline (**EBBA**) in the LC phases in a magnetic field on a glass plate treated with hexamethyldisilazane were investigated by POM. Those textures (Fig. 7b and c) are also dark, but there are 4-brushes and the brushes do not have bright areas at their centers. Thus, the texture of **F-BB-F** is quite different from those of **8CB** and **EBBA**. It is known that biaxial nematic phases exhibit three types of 1/2 disclinations (of both signs) corresponding to each director, and one $S = 1$ disclination[42] and the all-two-brush textures may not be the positive proof.[43] However, it is thought that the all-two-brush textures give us the possibility of the biaxiality.[2] The all-two-brush textures are also reported in papers of N_b phases in bent rod- and plate-like molecules.[11,14,44] It is assumed that this texture of **F-BB-F** originated from the lateral strong intermolecular face-to-face interaction.

Further, **F-FF-F** showed schlieren textures typical of nematic phases on applying a magnetic field (Fig. 7d). The texture has two- and four-brushes with broad lines. This also suggests that the PFA···A interaction is necessary to generate the all-two-brush textures, because **F-FF-F** molecules do not have intermolecular PFA···A interactions. Although we also tried a conoscopic study, we could not get a large enough area of the homeotropic thin-layered sample.

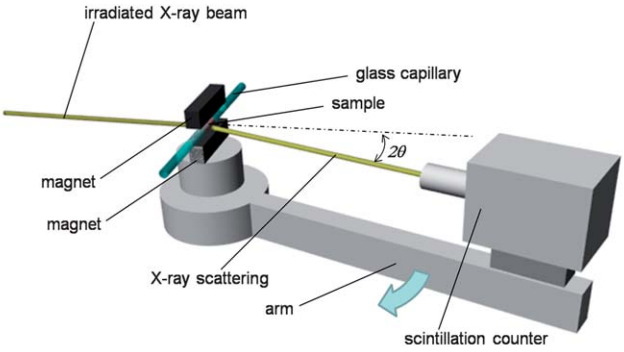

Fig. 8 Equipment for measuring the XRD of **F-BB-F** under a magnetic field. The X-ray beam irradiated the sample in a glass capillary which was set between a pair of magnets. The XRD intensity against the 2θ was measured. The angle ($\theta = 90°$) of the glass capillary to the irradiated X-ray beam was fixed.

We tried to measure homeotropically aligned textures of the smectic A phase of **F-BB-F** by applying a magnetic field. However, it was difficult to align the smectic A phase by using magnets to give the fan-shaped textures (Fig. S4†). Without applying a magnetic field, a homeotropically aligned part around the focal-conic was observed in some cases (Fig. S5†). However, it is very difficult to distinguish it from the usual homeotropic textures.

In order to investigate information on the repeat distances in the direction of the molecular short axis, the XRD profiles of **F-BB-F** in the isotropic liquid (290, 270 and 255 °C), nematic (240 and 210 °C), and smectic A (200 and 190 °C) phases were measured on applying a magnetic field. The equipment is depicted in Fig. 8. The LC sample was sealed in a glass capillary (ϕ = 1.5 mm), and a magnetic field (about 3500 gauss) was applied vertically to the glass capillary. The X-ray beam was irradiated horizontally to the LC sample, and the intensity of the X-ray diffraction against 2θ was measured by a scintillation counter. The XRD profiles are shown in Fig. 9. From the XRD profiles of the smectic A phases, it is clear that the rod-like molecules are well-aligned in parallel to the magnetic field because the large peaks of the inter-layer distances are not observed and the broad peaks based on the molecular widths are emphasized. In the isotropic liquid phase (270 and 255 °C), there is a small broad peak around 11.8 Å (2θ = 7.5°) corresponding to the d(200) reflection. The intensities of the broad peaks at wide angle region increased on cooling from the isotropic liquid to the nematic phase. At 240 °C (nematic phase), one broad peak at around 5.0 Å (b: 2θ = 17.5°) and one shoulder broad peak at 3.9 Å (a: 2θ = 22.5–23°) are observed. It is assumed that these two broad peaks correspond to two kinds of repeat distances in

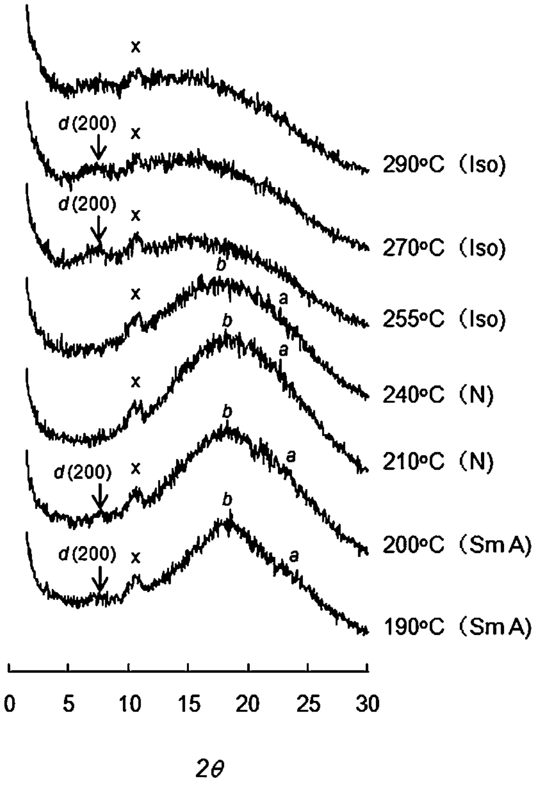

Fig. 9 XRD profiles of **F-BB-F** under a magnetic field showing broad peaks a, b and d(200) at 290 (Iso), 270 (Iso), 255 (Iso), 240 (N), 210 (N), 200 (SmA) and 190 (SmA) °C. Iso, N and SmA indicate isotropic liquid, nematic and smectic A phases, respectively. Peak x is a noise peak.

(a) Smectic A Phase (190°C)

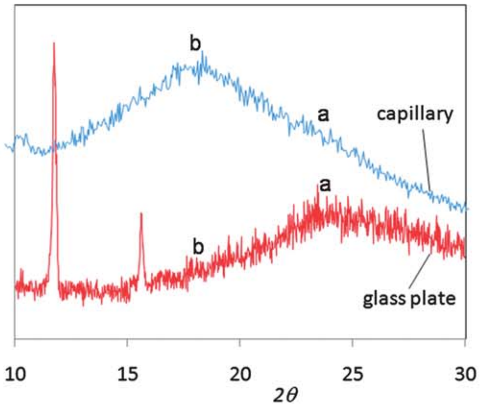

(b) Smectic A Phase (200°C)

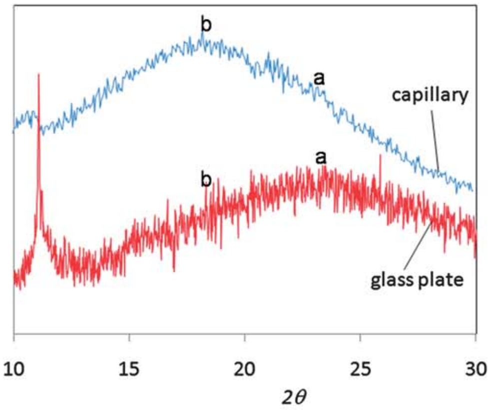

(c) Nematic Phase (210°C)

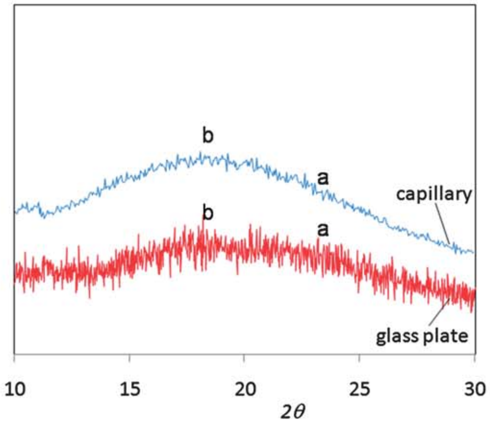

Fig. 10 XRD profiles of **F-BB-F** in the smectic A phase at (a) 190 °C and (b) 200 °C and nematic phase at (c) 210 °C under the following two experimental conditions: 1) capillary method in which the sample was packed in a glass capillary (ϕ = 1.5mm) and a magnetic field (3500 gaus) was applied (the profile was indicated by blue lines) and 2) glass plate method in which the sample was spread on a glass plate (the profile was indicated by red lines).

the lateral directions. At 210 °C (nematic phase), the peak at 5.0 Å (*b*: $2\theta = 18°$) and the shoulder peak at 3.9 Å (*a*: $2\theta = 22.5$–$23°$) were also observed. Lowering the temperature to 190 °C (smectic A phase), the broad peak (*b*: 5.0 Å, $2\theta = 18°$) became sharper and the broad shoulder peak *a* was also observed. These XRD profiles are compared with those measured using the glass-plate method (Fig. 10). In the smectic A phase both at 190 and 200 °C (Fig. 10a and Fig. 10b), the broad peak reached a maximum at 3.8–3.9 Å (peak *a*) and is emphasized in the glass-plate method. The molecules on the glass plate are more aligned in their lateral direction than those in the glass capillary. In the nematic phase (Fig. 10c), these two methods gave similar profiles. However, the shapes of these two profiles are slightly different. The profile of the glass-plate method includes the component of the broad peak (peak *a*) at 3.8–3.9 Å ($2\theta = 22.5$–$23°$) more than that of the capillary method.

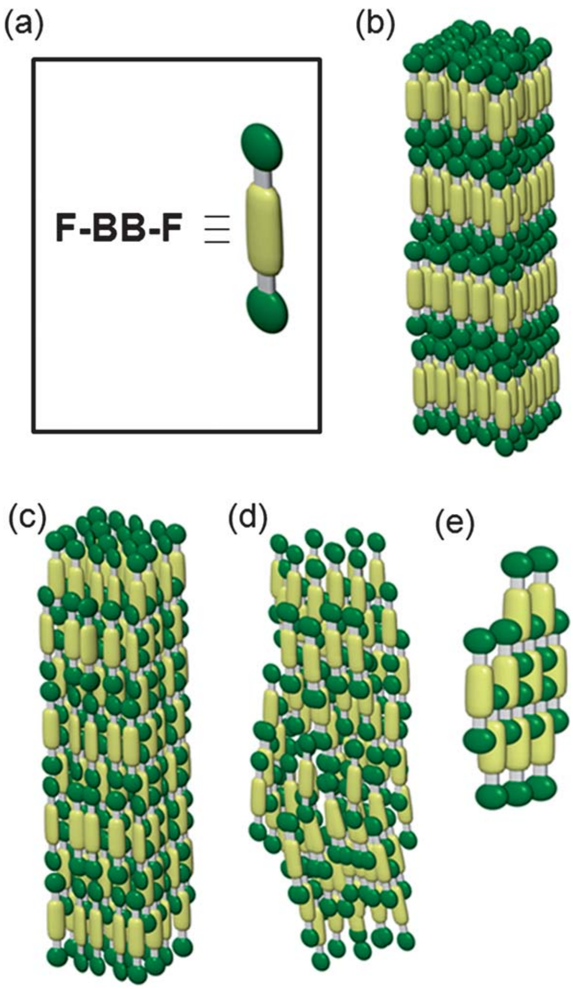

Fig. 11 Schematic representation of **F-BB-F** and its superstructures. (a) the molecular structure of **F-BB-F** and its schematic model, (b) layer structure ($d \approx l$, d: layer distance, l: molecular length) in the smectic A phase at 190 °C, (c) layer structure ($d \approx l/2$) in the smectic A phase at 200 °C, (d) the molecules in the nematic phases and (e) small molecular aggregate packed with a shift of the half molecular length in the nematic phase.

Estimation of the superstructures

From these results, the superstructures of **F-BB-F** in the smectic A and nematic phases were proposed as depicted in Fig. 11. In the smectic A phase of **F-BB-F**, it was suggested that the molecules were biaxially packed in the layers and the direction of their aromatic faces were controlled by the interaction with the glass surface. This means that the free rotation of the molecules around the long axes is suppressed on the glass plate and close to the glass surface as shown in Fig. 12a. In the low temperature region of the smectic A phase, it is expected that the PFBs and NFBs are micro-segregated as shown in Fig. 11b ($d \approx l$; d: layer distance; l: molecular length), which is similar to the molecular packing structure in the crystal. The edge-to-edge F···F interactions control the directions of the π-faces of the pentafluorophenyl groups and have a repeat distance of 3.8 Å. As the temperatures rise, molecular movements such as vibration and rotation increase, and the apparent volume of the terminal pentafluorophenyl groups increases compared to those of the biphenyl benzene rings. To minimize the intermolecular steric repulsions, the molecules are organized into a superstructure in which the molecules are packed with a shift of the half molecular length in the direction of the molecular long axes (($d \approx l/2$), Fig. 11c). In this superstructure, a face-to-face PFA···A interaction takes place between the molecules with a 3.9 Å π–π stacking distance (Fig. 12b). Thus, it is assumed that the equilibrium between the above-mentioned two superstructures in the smectic A phase is controlled thermodynamically. These lateral repeat distances 3.8–3.9 Å are very closed to the intercentroid distance 3.77 Å between benzene and hexafluorobenzene molecules in the cocrystal.[22] Though the nematic phase (Fig. 11d) does not show typical optical textures of layered structures, it is assumed that small clusters with the layer structures are laterally ordered (Fig. 11e) and are formed as observed in the 2D-XRD. Considering the observation of biaxiality in the smectic A phase in the 1D-XRD study, the results suggest that the molecules in the nematic phase are organized biaxially in the level of small

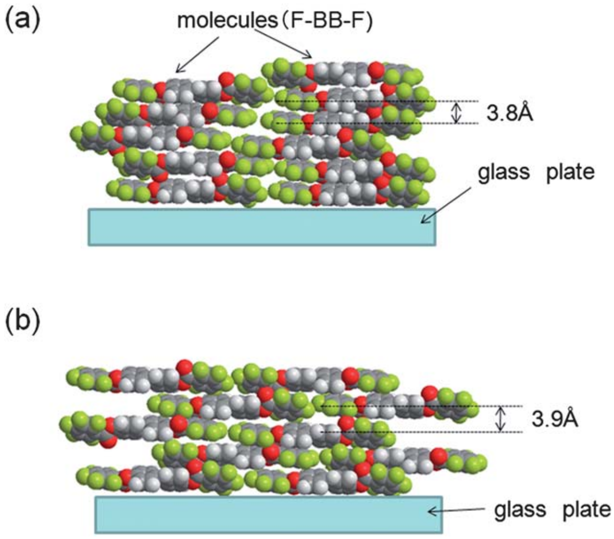

Fig. 12 Face-to-face molecular packing models (side view) of **F-BB-F** on the glass plate in the smectic A phases at (a) 190 and (b) 200 °C.

molecular aggregates by the strong lateral attractive face-to-face PFA···A interaction, which might be the origin of the schlieren textures with all-two-brush disclinations and of the difference between the 1D-XRD profiles of the glass plate and capillary methods.

Conclusions

In summary, we demonstrated that the simple non-alkylated rod-like molecules possessing PFBs and NFBs were self-organized to give stable mesophases by using F···F, CH···F and PFA···A interactions. Especially, compound **F-BB-F** consisting of a biphenyl moiety and two terminal pentafluorobenzoyl groups showed stable unique superstructures in its nematic and smectic A phases. The interlayer distances (*d*(200), *d*(300) and *d*(400)) were observed even in the nematic phase and the two XRD methods (glass plate and capillary methods) showed differences in the lateral repeat distances in both nematic and smectic A phases. For the stabilization of the liquid crystalline compounds possessing PFBs and NFBs, we emphasize that the following factors are important; 1) the 1 : 1 moiety ratio of PFBs and NFBs and 2) the flat molecular shape.

Experimental

Synthesis of 4,4′-bis(pentafluorobenzoyloxy)biphenyl (F-BB-F)

4,4′-Biphenol (0.30 g, 1.6 mmol), pentafluorobenzoic acid (0.68 g, 3.2 mmol), and dichloromethane (20 mL) were placed in a 100 mL round-bottom flask, and the mixture was cooled to 0 °C. To the mixture were added DMAP (0.02 g, 0.2 mmol) and DIPC (0.24 g, 1.9 mmol), and then the mixture was warmed to room temperature and stirred for 24 h. After quenching with 1 N HCl, the organic phase was washed with water (100 mL) and saturated $NaHCO_3$ (*aq.*) (50 mL), and dried over anhydrous sodium sulfate. The solvent was removed by evaporation. The residual crude product was purified by silica gel column chromatography eluting with chloroform/hexane (= 1 : 1).

F-BB-F

Yield 40%; ν_{max} (KBr)/cm^{-1} 3059, 1752, 1532, 1221, 1005; δ_H(400 MHz; $CDCl_3$; Me_4Si) 7.34 (d, *J* = 8.7 Hz, 4H), 7.65 (d, *J* = 8.7 Hz, 4H); δ_C(125.65 MHz; $CDCl_3$; Me_4Si) 121.70, 128.47, 138.79, 149.61, 157.52 (C=O) (The carbon atoms bearing a fluorine atom could not be observed); FT-HRMS (atmospheric pressure chemical ionization (ACPI)) 574.0247 (M^+. $C_{26}H_8F_{10}O_4$ requires 574.0257); EA ($C_{26}H_8F_{10}O_4$) calcd C 54.37, H 1.40, found C 54.21, H 1.11%.

Synthesis of 4-benzoyloxy-4′-(pentafluorobenzoyloxy)-biphenyl (F-BB-B)

4,4′-Biphenol (0.281 g, 1.51 mmol), benzoic acid (0.220 g, 1.80 mmol), and DMAP (18 mg, 0.15 mmol) were dissolved in dry THF (20 mL). DIPC (0.230 g, 1.82 mmol) was added into the solution with stirring. The solution was stirred at room temperature for 17 h. The reaction was quenched with 1 N HCl (20 mL). The solution was extracted with chloroform (20 mL × 3) and the combined organic solutions were dried over anhydrous sodium sulfate. After filtration, the solvent was removed by evaporation. The product was separated by silica gel column chromatography eluting with methanol/chloroform (= 1 : 9) to give 4-benzoyloxy-4′-hydroxybiphenyl as a white solid (0.240 g, 54.7%).

4-Benzoyloxy-4′-hydroxybiphenyl (0.14 g, 0.48 mmol), pentafluorobenzoic acid (0.12 g, 0.58 mmol), and dichloromethane (20 mL) were placed in a 100 mL round-bottom flask, and the mixture was cooled to 0 °C. To the mixture were added DMAP (0.01 g, 0.07 mmol) and DIPC (0.36 g, 0.29 mmol), and then the mixture was warmed to room temperature and stirred for 24 h. After quenching with 1 N HCl (20 mL), the organic phase was washed with water (100 mL) and saturated $NaHCO_3$ (*aq.*) (50 mL), and dried over anhydrous sodium sulfate. The solvent was removed by evaporation. The crude product was purified by silica gel column chromatography eluting with chloroform/hexane (= 1 : 1).

F-BB-B

Yield 80%; ν_{max} (KBr)/cm^{-1} 3066, 1750, 1732, 1496, 1219, 1004; δ_H(400 MHz; $CDCl_3$; Me_4Si) 7.31 (d, *J* = 8.7 Hz, 4H), 7.54 (t, *J* = 8.3 Hz, 4H), 7.65 (d, *J* = 8.7 Hz, 4H), 7.67 (t, *J* = 8.3 Hz, 2H), 8.24 (d, *J* = 8.3 Hz, 4H); δ_C(125.65 MHz; $CDCl_3$; Me_4Si) 121.60, 122.16, 128.27, 128.43, 128.62, 129.43, 130.22, 133.70, 137.86, 139.16, 149.45, 150.64, 157.53 (C=O), 165.20 (C=O) (The carbon atoms bearing a fluorine atom could not be; FT-HRMS (ACPI) 484.0729 (M^+. $C_{26}H_{13}F_5O_4$ requires 484.0718); EA ($C_{26}H_{13}F_5O_4$) calcd C 64.31, H 2.49, found C 64.47, H 2.71%.

Synthesis of 4,4′-bis(benzoyloxy)biphenyl (B-BB-B)

4,4′-Biphenol (0.50 g, 2.7 mmol), benzoic acid (0.82 g, 6.8 mmol), and dichloromethane (20 mL) were placed in a 100 mL round-bottom flask, and the mixture was cooled to 0 °C. To the mixture were added DMAP (0.06 g, 0.5 mmol) and DIPC (0.82 g, 6.4 mmol), and then the mixture was warmed to room temperature and stirred for 24 h. After quenching with 1 N HCl (20 mL), the organic phase was washed with water (100 mL) and saturated $NaHCO_3$ (*aq*) (50 mL), and was dried over anhydrous sodium sulfate. The solvent was removed by evaporation. The crude product was purified by silica gel column chromatography eluting with chloroform/hexane (=1 : 1).

B-BB-B

Yield 22%; ν_{max} (KBr)/cm^{-1} 3071, 1733, 1496, 1199, 1003; δ_H (400 MHz; $CDCl_3$; Me_4Si) 7.31 (d, *J* = 8.7 Hz, 4H), 7.54 (t, *J* = 8.3 Hz, 4H), 7.65 (d, *J* = 8.7 Hz, 4H), 7.66 (t, *J* = 8.3 Hz, 2H), 8.24 (d, *J* = 8.3 Hz, 4H); δ_C (125.65 MHz; $CDCl_3$; Me_4Si) 122.05, 128.23, 128.58, 129.45, 130.20, 133.65, 138.21, 150.42, 165.21 (C=O); FT-HRMS (ACPI): 393.1140 ($(M-1)^-$. $C_{26}H_{17}O_4$ requires 393.1121); EA ($C_{26}H_{18}O_4$) calcd C 79.17, H 4.60, found C 78.91, H 4.35%.

Synthesis of 4,4′-bisbenzoyloxyoctafluorobiphenyl (B-FF-B)

Octafluoro-4,4-biphenol (0.25 g, 0.75 mmol), benzoic acid (0.23 g, 1.90 mmol), and dichloromethane (20 mL) were placed in a 100 mL round-bottom flask, and the mixture was cooled to 0 °C. To the mixture were added DMAP (0.02 g, 0.2 mmol) and DIPC (0.23 g, 1.8 mmol), and then the mixture was warmed to room temperature and stirred for 24 h. After quenching with 1 N HCl (20 mL), the organic phase was washed with water (100 mL) and saturated $NaHCO_3$ (*aq*) (50 mL), and was dried over anhydrous sodium sulfate. The solvent was removed by evaporation. The crude product was purified by silica gel column chromatography eluting with chloroform/hexane (= 1 : 1).

B-FF-B

Yield 40%; ν_{max}(KBr)/cm^{-1} 3075, 1764, 1484, 1236, 1003; δ_H (400 MHz; $CDCl_3$; Me_4Si) 7.58 (t, $J = 8.3$ Hz, 4H), 7.73 (t, $J = 8.3$ Hz, 2H), 8.25 (d, $J = 8.3$ Hz, 4H); δ_C (125.65 MHz; $CDCl_3$; Me_4Si) 126.94, 128.94, 130.81, 134.48, 162.49 (C=O) (The carbon atoms bearing a fluorine atom could not be observed); FT-HRMS (ACPI): M^+ and $(M–1)^-$ were not observed; EA ($C_{26}H_{10}F_8O_4$) calcd C 58.01, H 1.87, found C 57.78, H 1.64%.

Synthesis of 4-benzoyloxy-4′-(pentafluorobenzoyloxy) octafluobiphenyl (F-FF-B)

Octafluoro-4,4′-biphenol (0.885 g, 2.68 mmol), benzoic acid (0.327 g, 2.68 mmol), and DMAP (33 mg, 0.27 mmol) were dissolved in dry THF (20 mL). DIPC (0.406 g, 3.22 mmol) was added into the solution with stirring. The solution was stirred at room temperature for 17 h. The reaction was quenched with 1*N* HCl (20 mL). The solution was extracted with chloroform (20 mL × 3) and the combined organic solutions were dried over anhydrous sodium sulfate. After filtration, the solvent was removed by evaporation. The product was separated by silica gel column chromatography eluting with methanol/chloroform (= 1 : 9) to give 4-benzoyloxy-4′-hydroxyoctafluorobiphenyl as a white solid (0.150 g, 12.9%).

4-Benzoyloxy-4′-hydroxyoctafluorobiphenyl (0.20 g, 0.46 mmol), pentafluorobenzoic acid (0.12 g, 0.55 mmol), and dichloromethane (20 mL) were placed in a 100 mL round-bottom flask, and the mixture was cooled to 0 °C. To the mixture were added DMAP (0.01 g, 0.01 mmol) and DIPC (0.06 g, 0.6 mmol), and then the mixture was warmed to room temperature and stirred for 24 h. After quenching with 1 N HCl (20 mL), the organic phase was washed with water (100 mL) and saturated $NaHCO_3$ (*aq*) (50 mL), and dried over anhydrous sodium sulfate. The solvent was removed by evaporation. The crude product was purified by silica gel column chromatography eluting with chloroform/hexane (= 1 : 1).

F-FF-B

Yield 80%; ν_{max} (KBr)/cm^{-1} 3041, 1765, 1495, 1235, 1004; δ_H (400 MHz; $CDCl_3$; Me_4Si) 7.32 (t, $J = 8.7$ Hz, 4H), 7.54 (t, $J = 8.3$ Hz, 2H), 7.65 (m, 5H), 8.24 (d, $J = 8.0$ Hz, 2H); δ_C (125.65 MHz; $CDCl_3$; Me_4Si) 126.94, 128.94, 130.81, 134.79, 162.36 (C=O of benzoyl) (the C=O carbon of the pentafluorobenzoyl and the carbon atoms bearing a fluorine atom could not be observed); FT-HRMS (ACPI): M^+ and $(M–1)^-$ were not observed; EA ($C_{26}H_5F_{13}O_4$) calcd C 49.70, H 0.80, found C 49.58, H 0.65%.

Synthesis of 4,4′-bis(pentafluorobenzoyloxy)octafluoro-biphenyl (F-FF-F)

Octafluoro-4,4-biphenol (0.25 g, 0.75 mmol), pentafluorobenzoic acid (0.40 g, 1.9 mmol) and dichloromethane (20 mL) were placed in a 100 mL round-bottom flask, and the mixture was cooled to 0 °C. To the mixture were added DMAP (0.02 g, 0.2 mmol) and DIPC (0.23 g, 1.8 mmol), and then the mixture was warmed to room temperature and stirred for 24 h. After quenching with 1 N HCl (20 mL), the organic phase was washed with water (100 mL) and saturated $NaHCO_3$ (*aq*) (50 mL), and dried over anhydrous sodium sulfate. The solvent was removed by evaporation. The crude product was purified by silica gel column chromatography eluting with chloroform/hexane (= 1 : 1).

F-FF-F

Yield 45%; ^{13}C NMR (125.65 MHz, $CDCl_3$, 25 °C): all carbon atoms could not be observed; ν_{max} (KBr)/cm^{-1} 1780, 1493, 1185, 1008 cm^{-1}; FT-HRMS (ACPI): M^+ and $(M–1)^-$ were not observed; EA ($C_{26}F_{18}O_4$) calcd C 43.48, H 0.00, found C 43.39, H −0.19%.

Single crystal data of F-BB-F

Chemical formula: $C_{26}H_8F_{10}O_4$, formula weight: 574.32, Temperature: 173 K, wavelength: 0.71073 Å, crystal system: monoclinic, space group: *C*2/*c*, Unit cell parameters: $a = 45.474(4)$ Å, $b = 7.4583(7)$ Å, $c = 6.3948(6)$ Å, $\beta = 91.1620(10)°$, $V = 2168.4(3)$ Å^3, $Z = 4$, D (calcd) = 1.759 mg m^{-3}, absorption coefficient: 0.175 mm^{-1}, $F(000) = 1144$, crystal size: 0.30 × 0.20 × 0.05 mm^3, crystal description: plate, crystal colour: no colour, theta range for data collection: 2.69 to 22.80°, index ranges: $-33 \le h \le 59$, $-9 \le k \le 9$, $-6 \le l \le 8$, independent reflections: 5939 [R(int) = 0.0304], absorption correction: empirical, max. and min. transmission: 0.9494 and 0.9913, refinement method: Full-matrix least-squares on F^2, data/restraints/parameters: 2496/0/198, goodness-of-fit: 0.928, final R indices [$I > 2$sigma(I)]: $R_1 = 0.0424$, $wR_2 = 0.1254$, R indices (all data): $R_1 = 0.0658$, $wR_2 = 0.1468$.

Acknowledgements

We are grateful to the Futaba Electronics Memorial Foundation, Mukai Science and Technology Foundation, the Asahi Glass Foundation for the funds, and we thank Grant-in-Aid for Scientific Research (B) 19350090.

Notes and references

1 G. R. Luckhurst, *Thin Solid Films*, 2001, **393**, 40; D. W. Bruce, *Chem. Rec.*, 2004, **4**, 10.
2 C. Tschierske and D. J. Photinos, *J. Mater. Chem.*, 2010, **20**, 4263.
3 B. K. Sadashiva, in *Handbook of Liquid Crystals, Vol. 2B: Biaxial Nematic LCs*, (ed.: D. Demus, J. W. Goodby, G. W. Gray, H.-W. Spiess and V. Vill), VCH, Weinheim, German 1998, pp. 933–943.
4 M. J. Freiser, *Phys. Rev. Lett.*, 1970, **24**, 1041.
5 R. Berardi, L. Muccioli and C. Zannoni, *J. Chem. Phys.*, 2008, **128**, 024905.
6 L. J. Yu and A. Saupe, *Phys. Rev. Lett.*, 1980, **45**, 1000.
7 C. C. Ho, R. J. Goetz and M. S. El-Aasser, *Langmuir*, 1991, **7**, 630; C. P. Bastos dos Santos and A. M. Figueiredo Neto, *Langmuir*,

1991, **7**, 2626; A. A. de Melo Filho, A. Laverde Jr. and F. Y. Fujiwara, *Langmuir*, 2003, **19**, 1127; E. F. Henriques, C. B. Passos, V. B. Henriques and L. Q. Amaral, *Liq. Cryst.*, 2008, **35**, 555.

8 L. V. Khoa, M. Mathews, M. Chambers, J. Harden, Q. Li, H. Takezoe and A. Jákli, *Phys. Rev. E*, 2009, **79**, 030701.

9 N. Vaupotič, J. Szydlowska, M. Salamonczyk, A. Kovarova, J. Svoboda, M. Osipov, D. Pociecha and E. Gorecka, *Phys. Rev. E*, 2009, **80**, 030701; B. Senyuk, H. Wonderly, M. Mathews, Q. Li, S. V. Shiyanovskii and O. D. Lavrentovich, *Phys. Rev. E*, 2010, **82**, 041711.

10 L. A. Madsen, T. J. Dingemans, M. Nakata and E. T. Samulski, *Phys. Rev. Lett.*, 2004, **92**, 145505; B. R. Acharya, A. Primak and S. Kumar, *Phys. Rev. Lett.*, 2004, **92**, 145506; C. V. Yelamaggad, S. K. Prasad, G. G. Nair, I. S. Shashikala, D. S. S. Rao, C. V. Lobo and S. Chandrasekhar, *Angew. Chem., Int. Ed.*, 2004, **43**, 3429; G. R. Luckhurst, *Angew. Chem., Int. Ed.*, 2005, **44**, 2834; V. Prasad, S.-W. Kang, K. A. Suresh, L. Joshi, Q. Wang and S. Kumar, *J. Am. Chem. Soc.*, 2005, **127**, 17224.

11 M. Lehmann, S.-W. Kang, C. Köhn, S. Haseloh, U. Kolb, D. Schollmeyer, Q. B. Wang and S. Kumar, *J. Mater. Chem.*, 2006, **16**, 4326.

12 L. Omnès, B. A. Timimi, T. Gelbrich, M. B. Hursthouse, G. R. Luckhurst and D. W. Bruce, *Chem. Commun.*, 2001, 2248; A. G. Vanakaras, M. A. Bates and D. J. Photinos, *Phys. Chem. Chem. Phys.*, 2003, **5**, 3700.

13 K. Praefcke, B. Kohne, D. Singer, D. Demus, G. Pelzl and S. Diele, *Liq. Cryst.*, 1990, **7**, 589; S. Chandrasekhar, G. G. Nair, D. S. S. Rao, S. K. Prasad, K. Praefcke and D. Blunk, *Liq. Cryst.*, 1998, **24**, 67; S. Chandrasekhar, G. G. Nair, D. S. S. Rao, S. K. Prasad, K. Praefcke and D. Blunk, *Curr. Sci.*, 1998, **75**, 1042.

14 S. Chandrasekhar, G. G. Nair, D. S. S. Rao, S. K. Prasad, K. Praefcke and D. Singer, *Mol. Cryst. Liq. Cryst.*, 1996, **288**, 7.

15 J. Malthête, H. T. Nguyen and A. M. Levelut, *J. Chem. Soc., Chem. Commun.*, 1986, 1548; J. Malthête, H. T. Nguyen, A. M. Levelut and Y. Galerne, *Compt. Rend. Acad. Sci. Paris*, 1986, **303**, 1073.

16 Q. M. Wang and D. W. Bruce, *Chem. Commun.*, 1996, 2505; Q. M. Wang and D. W. Bruce, *Angew. Chem., Int. Ed. Engl.*, 1997, **36**, 150.

17 J. J. Hunt, R. W. Date, B. A. Timimi, G. R. Luckhurst and D. W. Bruce, *J. Am. Chem. Soc.*, 2001, **123**, 10115; D. Apreutesei and G. H. Mehl, *Chem. Commun.*, 2006, 609; K.-U. Jeong, A. J. Jing, B. Mansdorf, M. J. Graham, D.-K. Yang, F. W. Harris and S. Z. D. Cheng, *Chem. Mater.*, 2007, **19**, 2921.

18 F. Hessel and H. Finkelmann, *Polym. Bull.*, 1986, **15**, 349; K. Saalwaechter and K. Severing, *Phys. Rev. Lett.*, 2004, **92**, 125501; K. Merkel, A. Kocot, J. K. Vij, R. Korlacki, G. H. Mehl and T. Meyer, *Phys. Rev. Lett.*, 2004, **93**, 237801; P. K. Karahaliou, P. H. J. Kouwer, T. Meyer, G. H. Mehl and D. J. Photinos, *J. Phys. Chem. B*, 2008, **112**, 6550.

19 B. K. Sadashiva, R. A. Reddy, R. Pratibha and N. V. Madhusudana, *Chem. Commun.*, 2001, 2140; T. Hegmann, J. Kain, S. Diele, G. Pelzl and C. Tschierske, *Angew. Chem., Int. Ed.*, 2001, **40**, 887; M. W. Schröder, S. Diele, N. Pancenko, W. Weissflog and G. Pelzl, *J. Mater. Chem.*, 2002, **12**, 1331; C. V. Yelamaggad, I. S. Shashikala, D. S. S. Rao, G. G. Nair and S. K. Prasad, *J. Mater. Chem.*, 2006, **16**, 4099.

20 C. R. Patrick and G. S. Prosser, *Nature*, 1960, **187**, 1021; J. H. Williams, *Acc. Chem. Res.*, 1993, **26**, 593; R. K. Castellano, F. Diederich and E. A. Meyer, *Angew. Chem., Int. Ed.*, 2003, **42**, 1210.

21 S. Lorenzo, G. R. Lewis and I. Dance, *New J. Chem.*, 2000, **24**, 295; O. R. Lozman, R. J. Bushby and J. G. Vinter, *J. Chem. Soc., Perkin Trans. 2*, 2001, 1446.

22 J. H. Williams, J. K. Cockcroft and A. N. Fitch, *Angew. Chem., Int. Ed. Engl.*, 1992, **31**, 1655.

23 F. Cozzi, F. Ponzini, R. Annunziata, M. Cinquini and J. S. Siegel, *Angew. Chem., Int. Ed. Engl.*, 1995, **34**, 1019; V. E. Williams, R. P. Lemieux and G. R. J. Thatcher, *J. Org. Chem.*, 1996, **61**, 1927; J. Hernandez-Ttrujillo, F. Colmenares, G. Cuevas and M. Costas, *Chem. Phys. Lett.*, 1997, **265**, 503; A. P. West, Jr., S. Mecozzi and D. A. Dougherty, *J. Phys. Org. Chem.*, 1997, **10**, 347; C. B. Martin, H. R. Mulla, P. G. Willis and A. Cammers-Goodwin, *J. Org. Chem.*, 1999, **64**, 7802.

24 C. B. Martin, B. O. Patrick and A. Cammers-Goodwin, *J. Org. Chem.*, 1999, **64**, 7807; F. Ponzini, R. Zagha, K. Hardcastle and J. S. Siegel, *Angew. Chem., Int. Ed.*, 2000, **39**, 2323; J. C. Collings, K. P. Roscoe, E. G. Robins, A. S. Batsanov, L. M. Stimson, J. A. K. Howard, S. J. Clark and T. B. Marder, *New J. Chem.*, 2002, **26**, 1740; M. Gdaniec, W. Jankowski, M. J. Milewska and T. Polonski, *Angew. Chem., Int. Ed.*, 2003, **42**, 3903; C. E. Smith, P. S. Smith, R. L. Thomas, E. G. Robins, J. C. Collings, C. Dai, A. J. Scott, S. Borwick, A. S. Batsanov, S. W. Watt, S. J. Clark, C. Viney, J. A. K. Howard, W. Clegg and T. B. Marder, *J. Mater. Chem.*, 2004, **14**, 413; T. M. Fasina, J. C. Collings, D. P. Lydon, D. Albesa-Jove, A. S. Batsanov, J. A. K. Howard, P. Nguyen, M. Bruce, A. J. Scott, W. Clegg, S. W. Watt, C. Viney and T. B. Marder, *J. Mater. Chem.*, 2004, **14**, 2395; J. C. Collings, J. M. Burke, P. S. Smith, A. S. Batsanov, J. A. K. Howard and T. B. Marder, *Org. Biomol. Chem.*, 2004, **2**, 3172; S. L. Cockroft, C. A. Hunter, K. R. Lawson, J. Perkins and C. J. Urch, *J. Am. Chem. Soc.*, 2005, **127**, 8594; M.-H. Yoon, A. Facchetti, E. S. Charlotte and J. M. Tobin, *J. Am. Chem. Soc.*, 2006, **128**, 5792; A. J. Mountford, S. J. Lancaster, S. J. Coles, P. N. Horton, D. L. Hughes, M. B. Hursthouse and M. E. Light, *Organometallics*, 2006, **25**, 3837; S. Bacchi, M. Benaglia, F. Cozzi, F. Demartin, G. Filippini and A. Gavezzotti, *Chem.–Eur. J.*, 2006, **12**, 3538; A. Hori, A. Shinohe, M. Yamasaki, E. Nishibori, S. Aoyagi and M. Sakata, *Angew. Chem., Int. Ed.*, 2007, **46**, 7617; F. Cozzi, S. Bacchi, I. Filippini, T. Pilati and A. Gavezzotti, *Chem.–Eur. J.*, 2007, **13**, 7177; F. Cozzi, S. Bacchi, G. Filippini, T. Pilati and A. Gavezzotti, *CrystEngComm*, 2009, **11**, 1122.

25 A. F. M. Kilbinger and R. H. Grubbs, *Angew. Chem., Int. Ed.*, 2002, **41**, 1563; S. S. Babu, V. K. Praveen, S. Prasanthkumar and A. Ajayaghoshi, *Chem.–Eur. J.*, 2008, **14**, 9577.

26 G. Mathis and J. Hunziker, *Angew. Chem., Int. Ed.*, 2002, **41**, 3203; S. M. Butterfield, P. R. Patel and M. L. Waters, *J. Am. Chem. Soc.*, 2002, **124**, 9751; G. Mathis, R. Schuetz and J. Hunziker, *Nucleosides, Nucleotides Nucleic Acids*, 2003, **22**, 1183; A. Zahn, C. Brotschi and J. C. Leumann, *Chem.–Eur. J.*, 2005, **11**, 2125.

27 K. B. Woody, J. E. Bullock, S. R. Parkin and M. D. Watson, *Macromolecules*, 2007, **40**, 4470.

28 S. K. Collins, Y. El-Azizi and A. R. Schmitzer, *J. Org. Chem.*, 2007, **72**, 6397.

29 T. Korenaga, Y. Kawauchi, T. Kosaki, T. Ema and T. Sakai, *Bull. Chem. Soc. Jpn.*, 2005, **78**, 2175.

30 T. Kato, N. Mizoshita and K. Kishimoto, *Angew. Chem., Int. Ed.*, 2006, **45**, 38; T. Kato, in *Handbook of Liquid Crystals, Vol. 2B: Hydrogen-bonded Systems*, (Eds; D. Demus, J. W. Goodby, G. W. Gray, H.-W. Spiess and V. Vill), Wiley-VCH, Weinheim1998, pp. 969–979.

31 C. Dai, P. Nguyen, T. B. Marder, A. J. Scott, W. Clegg and C. Viney, *Chem. Commun.*, 1999, 2493.

32 M. Weck, A. L. Dunn, K. Matsumoto, G. W. Coates, E. B. Lobkovsky and R. H. Grubbs, *Angew. Chem., Int. Ed.*, 1999, **38**, 2741.

33 K. Kishikawa, K. Oda, S. Aikyo and S. Kohmoto, *Angew. Chem., Int. Ed.*, 2007, **46**, 764.

34 H.-C. Weiss, R. Boese, H. L. Smith and M. M. Haley, *Chem. Commun.*, 1997, 2403; V. R. Thalladi, H.-C. Weiss, D. Bläser, R. Boese, A. Nangia and G. R. Desiraju, *J. Am. Chem. Soc.*, 1998, **120**, 8702; S. Tsuzuki, T. Uchimaru, M. Mikami and S. Urata, *J. Phys. Chem. A*, 2003, **107**, 7962; M. Horiguchi, S. Okuhara, E. Shimano, D. Fujimoto, H. Takahashi, H. Tsue and R. Tamura, *Cryst. Growth Des.*, 2008, **8**, 540; W. Caminati, J. C. Lopez, J. L. Alonso and J.-U. Grabow, *Angew. Chem., Int. Ed.*, 2005, **44**, 3840.

35 C. F. Matta, N. Castillo and R. J. Boyd, *J. Phys. Chem. A*, 2005, **109**, 3669.

36 M. Nishio, M. Hirota and Y. Umezawa, *The CH/ π interaction. Evidence, Nature and Consequences*; Wiley-VCH: New York, 1998; Y. Umezawa, S. Tsuboyama, H. Takahashi, J. Uzawa and M. Nishio, *Tetrahedron*, 1999, **55**, 10047; H. Abe and K. Miyamura, *Inorg. Chim. Acta*, 2000, **298**, 90; H. Suezawa, T. Yoshida, Y. Umezawa, S. Tsuboyama and M. Nishio, *Eur. J. Inorg. Chem.*, 2002, 3148; A. Matsumoto, T. Kunisue, S. Nagahama, A. Matsumoto, K. Sada, K. Inoue, T. Tanaka and M. Miyata, *Mol. Cryst. Liq. Cryst.*, 2003, **390**, 11; P. Thuery, T. G. Jeong and T. Yamato, *Supramol. Chem.*, 2003, **15**, 359.

37 R. Berardi and C. Zannoni, *J. Chem. Phys.*, 2000, **113**, 5971.

38 I. Dierking, *Texture of Liquid Crystals*, Wiley-VCH Verlag GmbH & Co. KGaA, Weinheim 2003.

39 A. D. Becke, *Phys. Rev. A: At., Mol., Opt. Phys.*, 1988, **38**, 3098; A. D. Becke, *J. Chem. Phys.*, 1993, **98**, 5648; C. Lee, W. Yang and R. G. Parr, *Phys. Rev. B*, 1988, **37**, 785; All DFT calculations were performed with Gaussian03; M. J. Frisch, *et al.*, *Gaussian R 03W, version 6.1*; Gaussian, Inc.: Pittsburgh, PA, 2004.

40 *Chem3D Ultra, Version 8.0* (Cambridge Soft Corporation).

41 A.-M. Levelut and M. Lambert, *Compt. Rend. Acad. Sci. (Paris)*, 1971, **272**, 1018; T. J. Dingemans, N. S. Murthy and E. T. Samulski, *J. Phys. Chem. B*, 2001, **105**, 8845.

42 Jakli and Saupe "*One- and two-dimensional Fluids*", 2006, Taylor & Francis, Boca Raton: p.185–187; V. P. Mineyev and G. E. Volovik, *Phys. Rev. B*, 1978, **18**, 3197.

43 J. R. Hughes, G. Kothe, G. R. Luckhurst, J. Malthête, M. E. Neubert, I. Shenouda and B. A. Timimi, *J. Chem. Phys.*, 1997, **107**, 9252; C. Chiccoli, I. Feruli, O. D. Lavrentovich, P. Pasini, S. V. Shiyanovskii and C. Zannoni, *Phys. Rev. E: Stat. Phys., Plasmas, Fluids, Relat. Interdiscip. Top.*, 2002, **66**, 030701.

44 S. Chandrasekhar, R. B. Ratna, B. K. Sadashiva and V. N. Raja, *Mol. Cryst. Liq. Cryst.*, 1988, **165**, 123; Y. Galerne, *Mol. Cryst. Liq. Cryst.*, 1998, **323**, 211.